



# Aerodynamic development of Formula Student race car

HENRIK DAHLBERG

Bachelor thesis at KTH Mechanics  
Supervisor: Stefan Wallin  
Examiner: Gustav Amberg



## **Abstract**

This thesis describes the process of developing the aerodynamics package of a Formula Student race car with computational fluid dynamics. It investigates the effects of aerodynamics on the vehicle's behaviour and performance with regard to the Formula Student competition format. The methods used during the development are evaluated and put into context by investigating the correlation between a wind-tunnel experiment of a wing in ground proximity, and its simulated counterpart. The aerodynamics package consists of an undertray, a front wing and a rear wing and the report details the stages involved in optimising these components to achieve the desired results.

## **Sammanfattning**

Denna avhandling beskriver processen att utveckla ett aerodynamikpaket för en Formula Student-bil med strömningsmekaniska beräkningar. Den undersöker effekterna av aerodynamik på fordonets beteende och prestanda med avseende på tävlingsformatet. De metoder som används under utvecklingen utvärderas och sätts i sitt sammanhang genom att undersöka hur väl ett vind-tunnelexperiment av en vinge nära marken korrelerar med dess simulerade motsvarighet. Aerodynamikpaketet består av ett golv, en främre vinge och en bakre vinge och rapporten detaljerar de steg som är involverade i att optimera dessa komponenter för att uppnå önskat resultat.

# Contents

<b>1</b>	<b>Introduction</b>	<b>1</b>
<b>2</b>	<b>Performance</b>	<b>2</b>
2.1	Top speed evaluation . . . . .	2
2.2	Cornering performance . . . . .	3
2.3	Load distribution . . . . .	3
<b>3</b>	<b>Tools</b>	<b>6</b>
3.1	XFLR5 . . . . .	6
3.2	ANSYS Workbench and FLUENT . . . . .	6
3.3	Design of Experiments . . . . .	6
3.4	ICEM CFD . . . . .	7
3.5	Autodesk Inventor . . . . .	7
<b>4</b>	<b>Verification of methodology</b>	<b>7</b>
4.1	Simulation of ground proximity experiment . . . . .	7
4.2	Mesh independence studies . . . . .	8
<b>5</b>	<b>Method</b>	<b>13</b>
5.1	Multi-element aerofoil development . . . . .	14
5.2	Undertray and diffuser development . . . . .	16
5.3	Wing simulation . . . . .	21
<b>6</b>	<b>Acknowledgements</b>	<b>24</b>



# 1 Introduction

Aerodynamics have been a major subject in racing for the past 40 years with the purpose of increasing the normal load on the tires for increased grip without the corresponding addition of mass. The amount of grip available in the tires along with aerodynamic drag and engine power set the theoretical limits for the vehicle's velocity around the track, especially in cornering, and it is thus of particular interest when designing a vehicle to increase this grip while keeping drag to a minimum. Over the years, rules and regulations have been imposed to keep these aerodynamic advantages on a reasonable scale as technology has improved.

In the design of an open-wheel formula race car, one is faced with numerous instances of complex geometry; rotating wheels, A-arms and the cockpit with a driver to name a few. This nature of the vehicle make it difficult if not impossible to approach the problem of aerodynamic optimization of the entire car analytically. It is due to these difficulties that methods of simulation such as computational fluid dynamics (CFD) have been developed to aid the research and it is the objective of this thesis to develop the aerodynamic package of a Formula Student race car complete with front and rear wing, undertray and diffuser using CFD.



Figure 1: The KTH Racing R3 vehicle with the team's first aerodynamics package

Formula Student is the European version of the American Formula SAE competition [9]. It is an engineering competition in which students design and build and open wheeled race car. The purpose is to produce a race car prototype to be evaluated for production. Competing cars from different teams will be judged to determine the best overall car in terms of, among others, cost, reliability and performance. Formerly KTH Racing, KTH Formula Student is the team at KTH, involving 30-50 students each year. The team has existed since 2004 and have since then gone from manufacturing combustion vehicles to electric vehicles.

The competition is held every summer in different parts of Europe, the most

popular competitions being in England and Germany. Formula Student has static and dynamic competition events. Static events include manufacturing, cost and design. The teams are required to demonstrate their engineering, marketing and manufacturing knowledge. The dynamic events test the cars performance in different scenarios such as acceleration, autocross and endurance.

The most notable work performed earlier in the field of Formula Student aerodynamics was published in a series of papers by S. Wordley and J. Saunders in 2006 ([5], [6]) and their work has served as a great inspiration to this project. KTH Racing also developed an aerodynamics package for the KTH R3 vehicle in 2006. The rules back then looked different from today however and it is the hope of the author of this thesis to develop a package of the same quality in the modern format.

## 2 Performance

### 2.1 Top speed evaluation

One of the drawbacks to adding an aerodynamics package with wings to a race car is the added amount of drag. It is important to evaluate the effect of drag on the vehicles top speed as to determine how much we can afford without sacrificing on-track performance. The competition tracks are designed for a limited velocity and thus we can investigate if the added drag is believed to limit the velocity more than desired.

The acceleration of the car can be described simply as

$$m\ddot{x} = F - \frac{1}{2}\rho C_D A \dot{x}^2 \quad (1)$$

where  $F$  is the force driving the vehicle forward,  $\rho$  is the density of air,  $C_D$  is the drag coefficient and  $A$  is the reference frontal area. The rolling resistance has been ignored here. When equilibrium between the driving force and the drag force is reached, the acceleration  $\ddot{x}$  is zero and (1) simplifies to

$$F = \frac{1}{2}\rho C_D A \dot{x}^2. \quad (2)$$

The driving force can be expressed in terms of the engine power  $P$  and the car velocity  $v = \dot{x}$ . As described by McBeath in [2], this approximately yields

$$P = \frac{C_D A v^3}{1.633}. \quad (3)$$



For a rough estimation of the drag limitation on top speed we use some realistic values for the vehicle data. With an engine power  $P = 85 \text{ kW}$ , drag coefficient  $C_D = 0.85$  and frontal area  $A = 0.9 \text{ m}^2$ , the theoretical top speed is  $v_{max} = 203.8 \text{ km/h}$ . Since the tracks at the competitions are designed for maximum velocities of  $\sim 110 \text{ km/h}$ , we can calculate the maximum allowed  $C_D$  with the new frontal area after the addition of a rear wing. Assuming a desired top speed of  $v = 125 \text{ km/h}$  in order to allow for some margin, and a new frontal area of  $A = 1.2 \text{ m}^2$ , the highest allowed drag coefficient is  $C_{D_{max}} = 2.76$ . This is a very high drag coefficient, and this indicates that the induced drag from the added aerodynamics package is not likely to limit the top speed of the vehicle to a degree that it would hurt its performance for its intended purpose.

## 2.2 Cornering performance

One of the major benefits to equipping a race car with an aerodynamics package is the increased grip in the tyres. The increase in performance due to the extra grip from the added normal load can be investigated and demonstrated by inspecting the theoretical maximum allowed velocity in cornering before the vehicle loses its grip. This is the velocity for which the frictional force is equal to the centripetal force. Assuming constant coefficient of friction we have

$$\mu F_z = \mu \left( mg + \frac{1}{2} \rho C_L A v^2 \right) = \frac{mv^2}{R} \quad \Leftrightarrow \quad v = \sqrt{\frac{mg}{m/\mu R - \frac{1}{2} \rho C_L A}},$$

where  $m$  is the car mass,  $g$  the gravitational acceleration,  $\mu$  the coefficient of friction,  $\rho$  the density of air,  $C_L$  the lift coefficient,  $A$  the reference frontal area and  $R$  the corner radius. The rules of the competition state that the tracks in the different events have corners with radii varying from 4 m to 30 m [7]. The maximum cornering velocity with a lift coefficient of the entire car of  $C_L = 1.7$  is plotted together with the velocity without downforce versus the range of  $R$  encountered at the competition.

## 2.3 Load distribution

In order to achieve the desired load distribution from the aerodynamic forces, one must take the positions and dimensions of the wings into consideration. It is the desire of the KTH Formula Student team to keep the aerodynamic load center close to the center of gravity ( $CG$ ) to maintain similar handling characteristics at different velocities. This motivation is supported by the fact that the team is prohibited from using professional drivers at the competition who may otherwise be more capable of

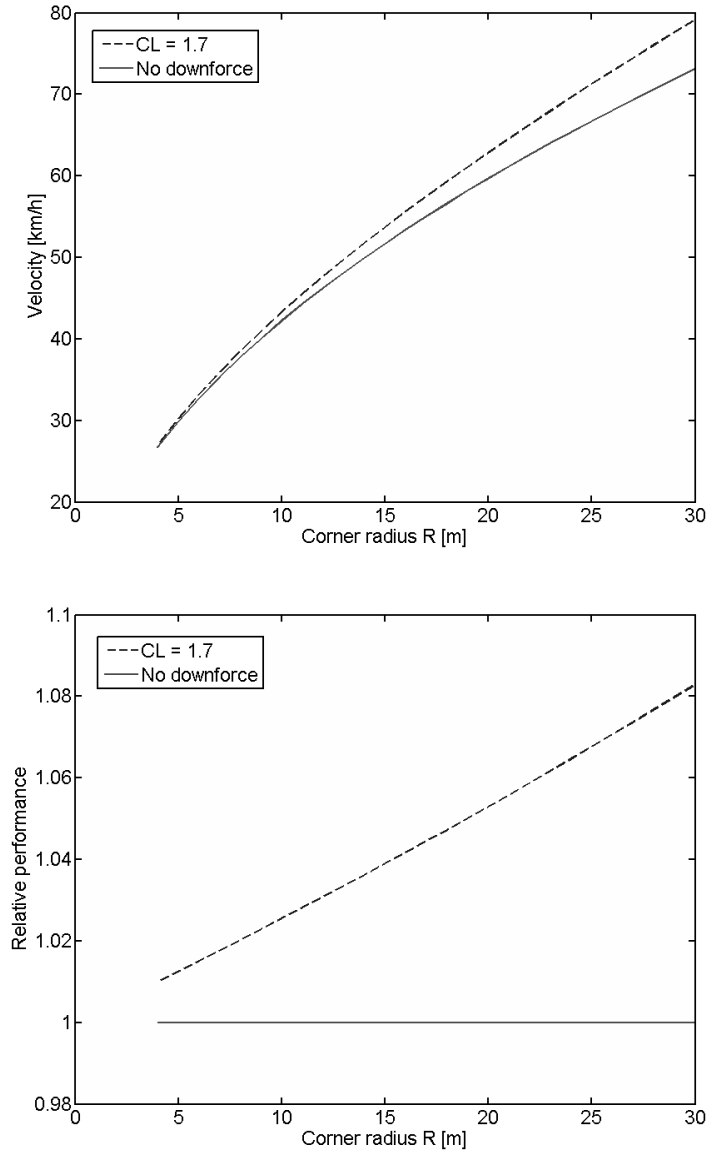


Figure 2: Absolute and relative velocities with and without downforce

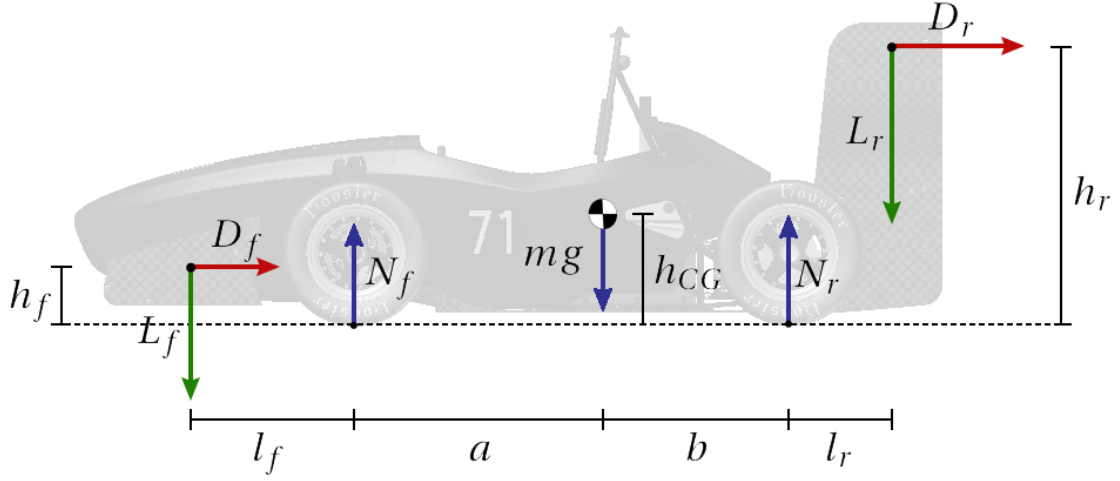


Figure 3: Free body diagram of forces acting on the vehicle

handling a vehicle with more intricate behaviour. With this in mind and assuming that the downforce generated from the undertray acts on a point close to  $CG$ , the load on the rear tyres can be calculated using equilibrium considerations on a free body diagram of the forces acting on the vehicle.

$$\begin{aligned}
 \uparrow: \quad \sum_i \mathbf{e}_z \cdot \mathbf{F}^{(i)} &= 0 & \Rightarrow & \quad N_f + N_r - mg - L_f - L_r = 0 \\
 \curvearrowright: \quad \sum_i (\mathbf{r}^{(i)} - \mathbf{r}_{CG}) \times \mathbf{F}^{(i)} &= \mathbf{0} & \Rightarrow & \quad bN_r - aN_f - (l_r + b)L_r + (l_f + a)L_f \\
 & & & \quad + (h_{CG} - h_r)D_r + (h_{CG} - h_f)D_f = 0
 \end{aligned}$$

This gives the force on the rear tyres as

$$N_r = \frac{amg + (l_r + a + b)L_r - l_fL_f + (h_r - h_{CG})D_r + (h_f - h_{CG})D_f}{a + b}$$

which can be used to calculate the total load distribution for the aerodynamic forces at different velocities.

## 3 Tools

### 3.1 XFLR5

XFLR5 is an aerofoil analysis tool. It uses the XFOIL code developed by Mark Drela at MIT. In this project it was used to compare characteristics of different aerofoils during the initial stages of the multi-element aerofoil optimisation.

### 3.2 ANSYS Workbench and FLUENT

ANSYS Workbench is an engineering software suite, equipped with many different solvers and project management utilities. It was the main toolbox for this project, used to organize the modelling, meshing, solving and post-processing parts of the different optimisations and simulations.

FLUENT is the CFD solver used in this project. It is included in the Workbench suite which allows for a smoother work-flow. Most of the knowledge about using this software has been acquired in a learn-by-doing approach, and the procedures used have been derived from the best practice guidelines found in [11].

### 3.3 Design of Experiments

Design of Experiments (DoE) is the exercise of designing an experiment so that relevant data can be properly extracted. For this project, the built-in DoE tools in ANSYS Workbench was used to find the set of parameters that should be tested and simulated in order to find the best configuration. Since the amount of available configurations grow very large when more than a few parameters are involved, a DoE approach is a comfortable time saving method.

The type of DoE used for the optimisations in this project is central composite design (CCD). This defines a set of points in the parameter space and runs the simulations for these points. As the optimisations are expected to have strongly non-linear behaviour, the use of a Kriging response surface with automatic refinement is suggested by ANSYS. This will solve for points in the parameter space and improve the response surface by adding more configurations to test automatically. Once an acceptable response surface with a predicted relative error of less than 5% is created, the optimal configuration for a given design parameter can be found.

### 3.4 ICEM CFD

Apart from the standard meshing capabilities in ANSYS Workbench, ICEM CFD was used in meshing more complex 3D geometries as it offers more control over the meshing procedure.

### 3.5 Autodesk Inventor

Autodesk Inventor is the CAD program used by the KTH Formula Student team. It was used to design all the geometries for the aerodynamics package before being imported and pre-processed in ANSYS DesignModeler.

## 4 Verification of methodology

### 4.1 Simulation of ground proximity experiment

In order to determine the usefulness of the methods used for the simulations in this thesis, and how well they are able to simulate real aerodynamic flows, the experiment of a wing in ground proximity conducted by X. Zhang and J. Zerihan in [8] was simulated in ANSYS Fluent. Some uncertainties were involved. The operating conditions in the wind tunnel was unknown and was assumed to be atmospheric. The wing end plate dimensions were known, but not their exact placement relative to the wing elements, and were thus placed to resemble the pictures in the report as closely as possible. The 2D simulations were run for mesh sizes of  $\sim 150,000$  nodes. In order to run the 3D simulations on a portable personal computer in a reasonable time frame, the mesh size was limited to  $\sim 6,000,000$  cells.

The 3D simulations show a slight deviation from the experimental data for low ground clearance. The 3D simulation is fully turbulent while the flow in the experiment was partially laminar, which among other uncertainties may be the cause to the deviations in the results. It was concluded that 3D simulations can be used to get results accurate enough for the development of an aerodynamics package. The results show that the 2D simulations strongly overestimate the wing lift coefficient, but they give an indication of where the maximum can be achieved and may thus still be useful for time efficient investigations.

A comparison of the velocity and pressure contours of the 2D simulation and the 3D simulation in the symmetry plane and close to the end plate for a ground clearance of 17.1 mm is shown. The contours of the 2D case and the symmetry plane in the 3D case are reasonably similar, but the contours in the plane close to the

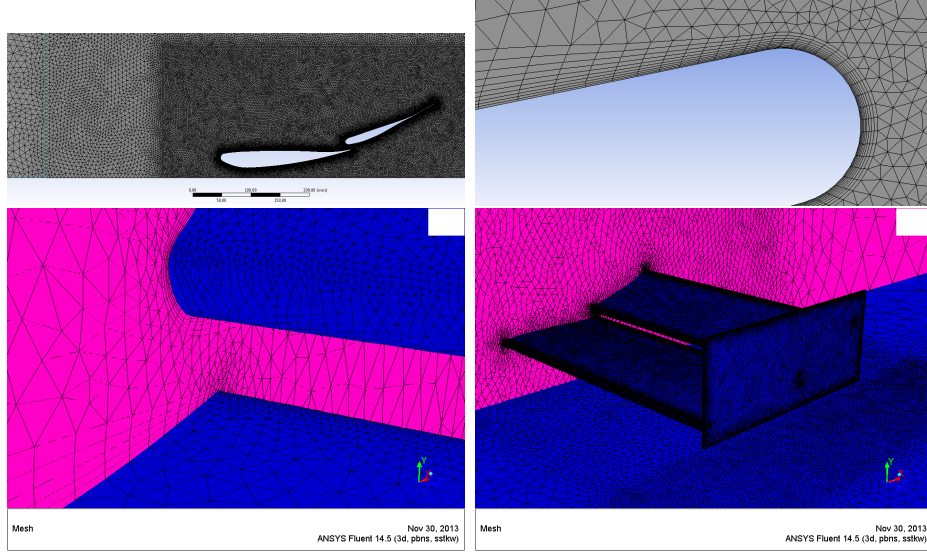


Figure 4: 2D and 3D meshes for ground proximity simulations

end plate shows that the flow is heavily influenced by 3D effects such as end plate vortices.

Lastly, surface streamlines coloured by wall shear from simulations is shown together with oil flow visualisation from [8] on the wing suction surface for a ground clearance of  $\sim 81$  mm. The differences in areas of laminar and turbulent flow may be a contributing factor to the deviations in lift.

## 4.2 Mesh independence studies

To determine that the solutions will be fully converged and not dependent of the mesh resolutions, mesh independence studies were conducted. One such study was made on a geometry that represented a typical multi-element aerofoil that was to be optimised. It was done by uniformly refining the mesh throughout the domain and observing how the calculated lifting force changed with the increasing amount of nodes. The settings with the lowest node count that still yielded results within acceptable margins was then used in the optimisation of the aerofoil, as well as in the optimisation of the tunnel profile of the undertray and during the simulation of the wind-tunnel experiment described previously. This procedure will ideally give results that are accurate enough while keeping the computation times to a minimum.

Ideally one would like to conduct a similar study for the 3D simulations as well. With the computation power available this was however not a feasible option with

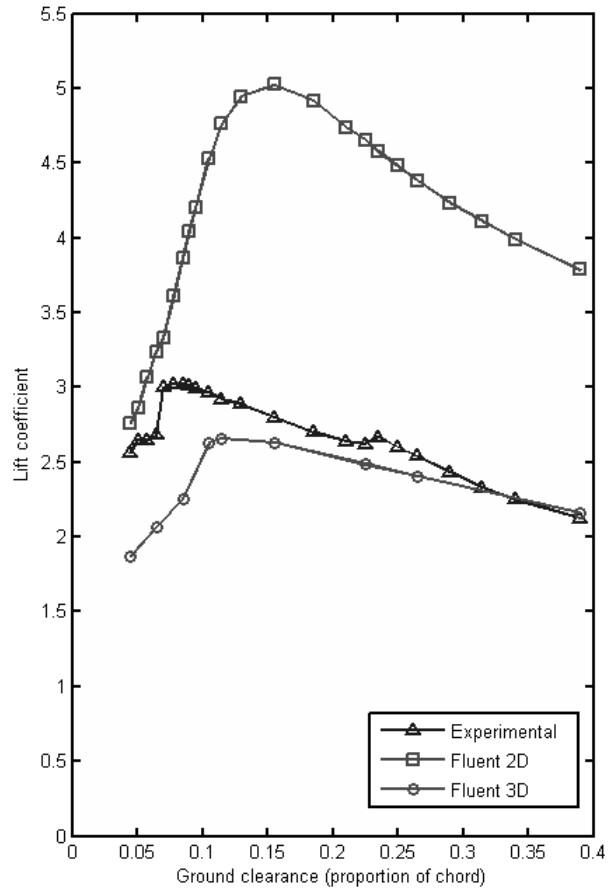


Figure 5: Results of the ground proximity simulations

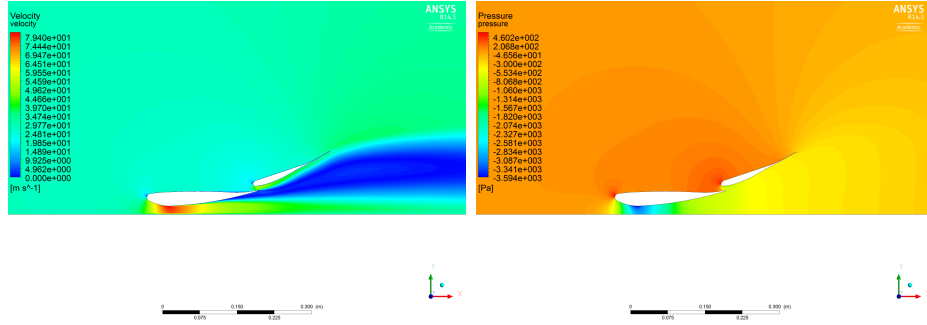


Figure 6: 2D velocity and pressure contours

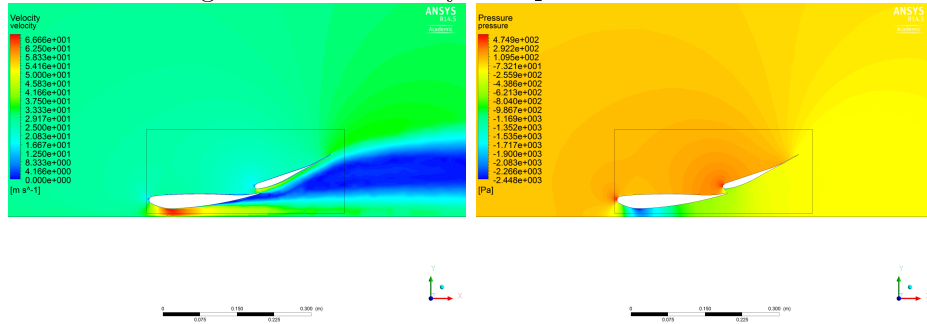


Figure 7: 3D velocity and pressure contours, symmetry plane

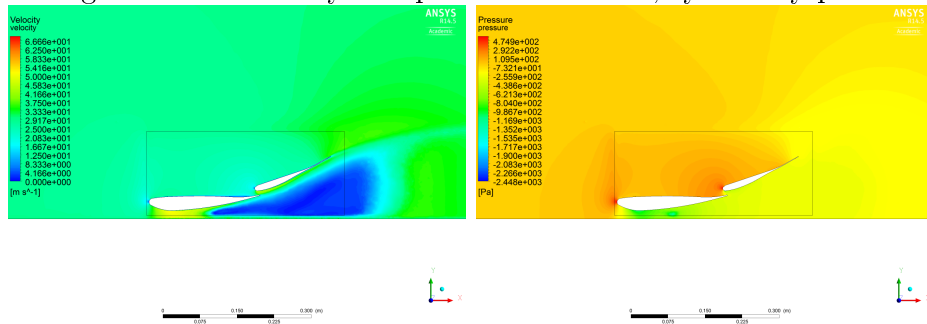


Figure 8: 3D velocity and pressure contours, near end plate



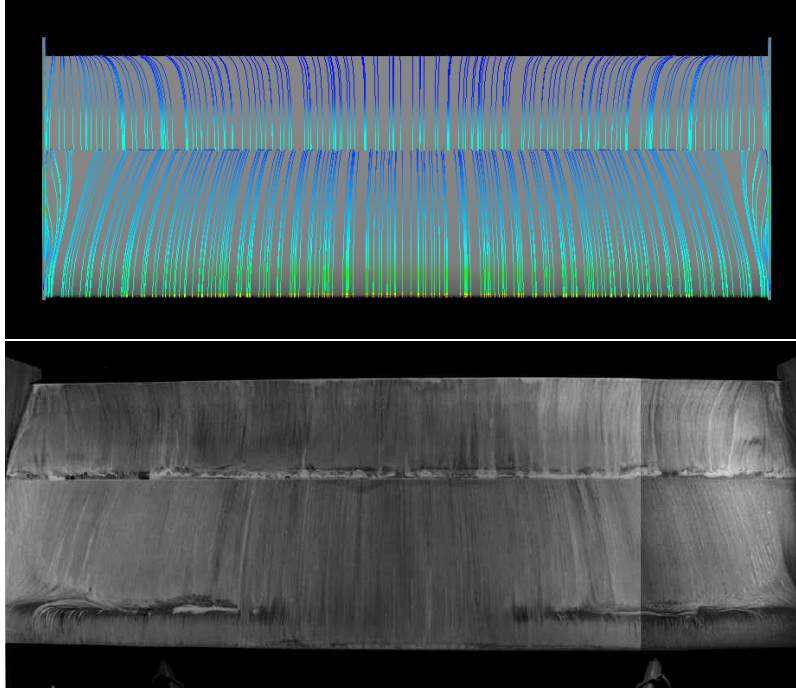


Figure 9: Simulated surface streamlines compared to experimental oil flow visualisation

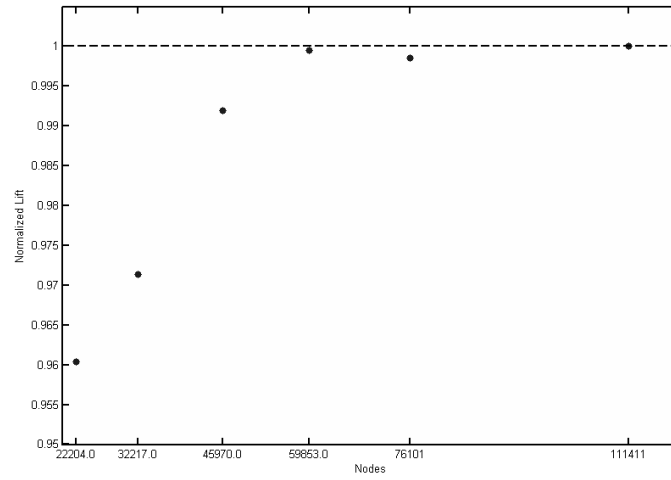


Figure 10: Results of the mesh independence study on the multi-element aerofoil

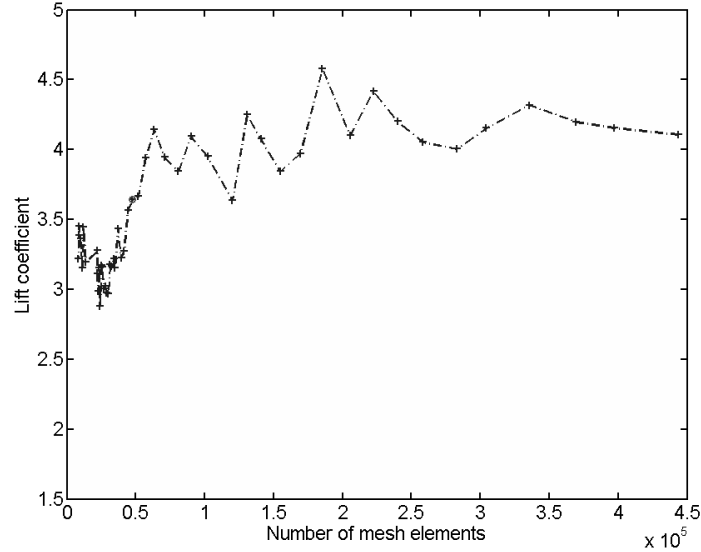


Figure 11:  $C_l$  convergence for uniformly refined meshes of the front wing cut-section

regard to time. Instead, the strategy was to select a cut-section of a 3D mesh that was small enough to be handled by the computer, in this case a mesh of the vehicle's front wing with a coord of  $\sim 700$  mm, and perform the study on the 2D mesh of that cut-section. This study was done two ways, one with uniform refinement as with the multi-element aerofoil previously, and the other with  $y^+$  adaptation in FLUENT. With the first method, the mesh sizes were set as in the 3D mesh and then coarsened or refined linearly with a scalar parameter, which resulted in more coarse or fine mesh in the entire domain. The mesh used in the 3D case corresponds to a 2D mesh of  $\sim 60,000$  elements. The second method was to use three variations of the original mesh, here named Coarse, Medium and Fine, each with 6 mm, 1.5 mm and 0.375 mm element sizes respectively on the wing wall. These meshes were then gradually refined with mesh adaptation in Fluent step by step for different values of  $y^+$ , after the simulations had converged in each step. The meshes for the second method thus had the same element sizes in the free flow regions as the 3D mesh, but refined elements in the boundary layers.

The results from the first method with uniform mesh refinement seems to converge slowly but the element count grows very large as the entire domain is refined. Taking the results from the second method with refinement by  $y^+$ -adaptation into account, we see that refinement in the boundary layer seems enough to get convergence and

$y^+$	Coarse	Medium	Fine
-	3.05	3.84	4.20
30	3.06	3.93	4.26
15	3.16	3.94	4.18
10	3.54	3.89	4.07
5	3.71	4.02	4.06

Table 1:  $C_l$  for different meshes of the front wing cut-section with gradual  $y^+$  adaptation in FLUENT

comparing to the first method we see that the results are independent of refinement in the other areas of the domain. The Fine mesh with  $y^+ = 5$  consisted of less than 200,000 elements which is a substantially lower element count than the finer meshes from the uniform refinement in the first method. Due to the difficulties of creating a well-resolved boundary layer mesh for geometries like these, it was thus convenient to use  $y^+$ -adaptation in FLUENT in the 3D simulations of the full vehicle to increase the likelihood of getting mesh-independent results while saving time.

## 5 Method

The development of the aerodynamics package consisted of several stages. The first stage was to develop an aerofoil configuration capable of producing high downforce, as it was established early that the drag would not be a major concern. It was expected that the undertray would have a very small, perhaps negligible effect on the load distribution of the vehicle, and thus it was designed after the aerofoil configuration before the front and rear wing was introduced, as these would clearly affect the balance. The front wing does influence the performance of the undertray, but this is something one can not avoid and optimising these parts in relation to each other is beyond the scope of this project. When the undertray design was established, the strategy was to design the front wing to produce as much downforce as possible while complying with the competition rules for wing size and clearance to the wheels and the ground. The respective rules for the rear wing allow it to be sized and positioned so that the downforce it produces is not as limited as with the front wing, and therefore it can be designed in the final stage of the process to achieve the desired aerodynamic load distribution while maximizing downforce.

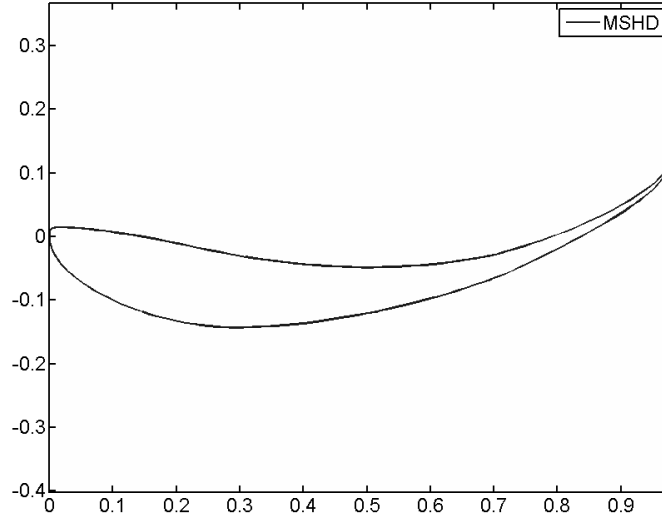


Figure 12: MSHD aerofoil

## 5.1 Multi-element aerofoil development

A multi-element aerofoil was developed to be used for the front and rear wing of the vehicle. A selection of five aerofoils were analysed in the XFLR5 software to determine a suitable candidate the multi-element configuration.

- Eppler E423
- Douglas/Liebeck LNV109A
- NACA 7412
- Selig S1223
- MSHD

The aerofoils were chosen due to their high lift characteristics. The MSHD aerofoil was developed specifically for the Formula Student competition [1] and the rest were retrieved from the UIUC Airfoil Coordinates Database [10]. Batch simulations were run for each aerofoil over a set span of angles of attack. It was evident that the MSHD aerofoil had a desirable high lift coefficient, however the long thin section connected to the trailing edge bring difficulties with manufacturing. This lead to the decision to develop the multi-element aerofoil with a the less aggressive profile 'Eppler' E423, which shares similar lift characteristics with the MSHD aerofoil.

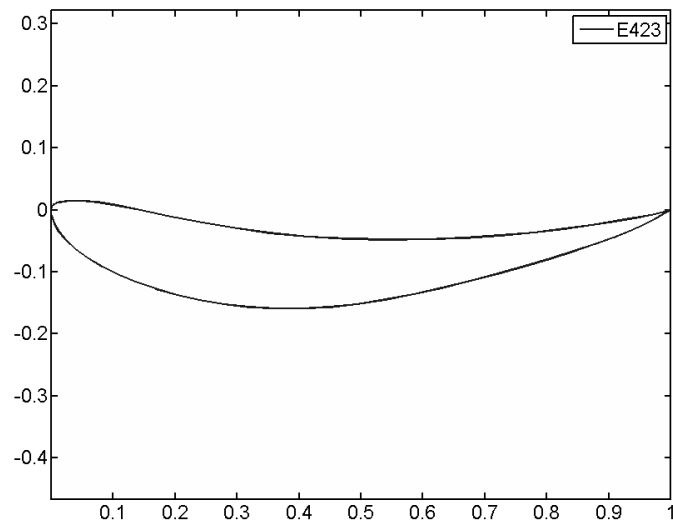


Figure 13: E423 aerofoil

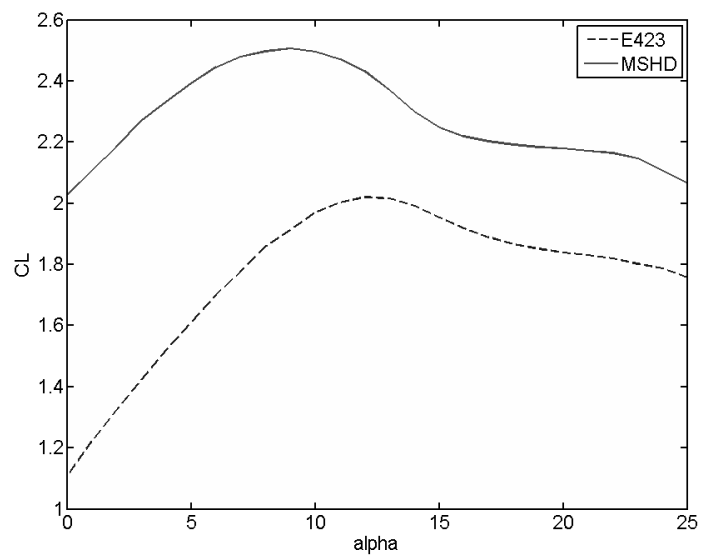


Figure 14: Lift curve for the MSHD and E423 aerofoils

The first approach to optimising the aerofoil was to make an initial guess based on suggestions in literature ([2], [3]). To limit the complexity of the optimisation, it was decided that an aerofoil consisting of three elements, all with the same profile, should be optimised, as this has historically been a successful way of generating a high downforce aerofoil [3]. Batch simulations were run in which different parameters such as flap sizes, angles and distances were varied. Due to the many variables involved in such an optimisation, the number of available configurations grow very large, making for an uncomfortable analysis. In an attempt to reduce this number, the aerofoil angle of attack was fixed at an angle of  $\sim 25^\circ$  where the configurations were expected to operate close to their maximum. It was learned however that this method causes the aerofoil  $C_l$  to be optimised for that specific angle of attack, while performing poorly for others, introducing heavy separation. A discontinuity in the lift curve was present which made it evident that some other method should be used to optimise the aerofoil configuration in a more efficient manner while avoiding this unacceptable behaviour.

This mistake from the first round of optimisation was remedied by taking a new approach, limiting the flap angles and re-running the optimisation of the other parameters with the DoE tools available in ANSYS Workbench. This way the tool itself would find configurations to simulate in order to find sufficient information about where the maximum may be. The resulting aerofoil configuration has a wide operating range which allows the wings to work properly despite changes in angle of attack that occur when driving around a race track.

## 5.2 Undertray and diffuser development

The optimisation of an entire undertray for a formula-style race car is a time consuming process with many affecting parameters. There are many ways to design a race car undertray that produces some downforce, and the choice mostly comes down to packaging of the rest of the vehicle's components. An undertray with double tunnel design seemed to fit our needs the best. It was decided that the optimisation of the tunnel profiles should be carried out using DoE tools similar to the aerofoil optimisation. The tunnels consists of an inlet, a throat section and a diffuser. The inlet height, and diffuser height was set as parameters in the DoE optimisation. The throat section was defined with two parameters, the height at the front and rear points, to allow for optimisation of the tunnel inclination. The rest of the dimensions such as the length of the inlet, throat and diffuser were fixed due to geometry and competition rule constraints. A blunt body was used to simulate blockage above the tunnel.

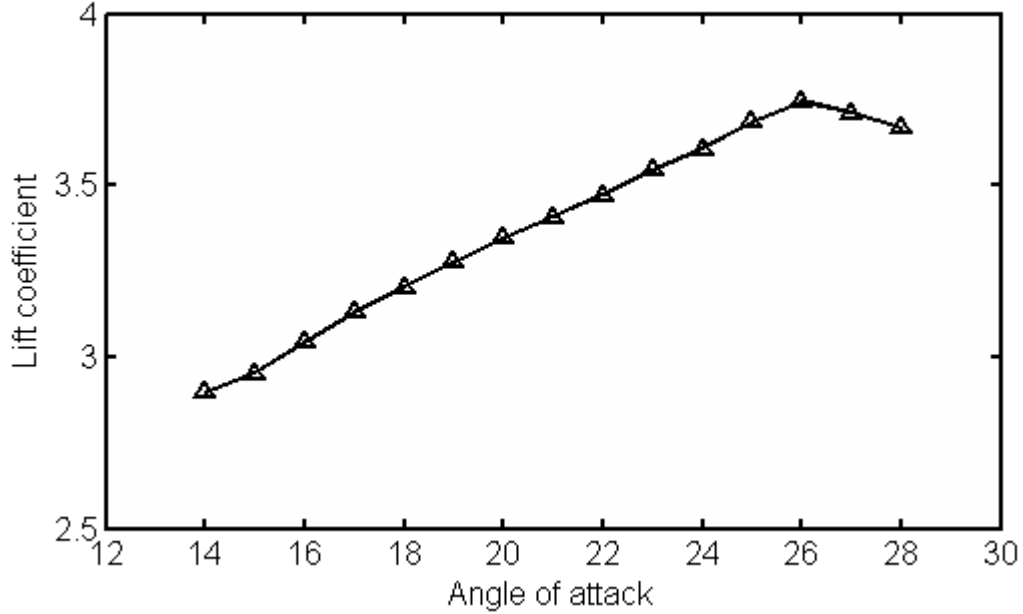


Figure 15: Lift curve for optimised aerofoil configuration

The optimal solution found during the DoE optimisation of the tunnel profile was used to make an initial design of the undertray with its two tunnels. This was then simulated in absence of the main bodywork and wheels. The undertray was then integrated to the main body for the rest of the simulations, and a splitter was added in the front to help streamline the flow.

In the second design iteration the tunnels were made more narrow due to packaging issues that came along during development. A flat floor section was extended in front of the added splitter to allow for mounting to the frame. This second revision was then simulated together with the main bodywork. The mesh cell count grew larger than the previous case due to the added geometry, but the same mesh sizing and solver settings were used. It is difficult to assess the performance of the undertray as one would have to compare the downforce of the entire body with undertray to just the body without it.

It was observed that the proximity of the wheels influenced the airflow negatively, especially in the rearmost part of the tunnels, and in the final iteration a few vertical separating walls were added in an attempt to keep the flow clean. Undoubtedly the development of the undertray could be taken further, but the optimisations involved are intricate and there are many options to consider. Further development was thus

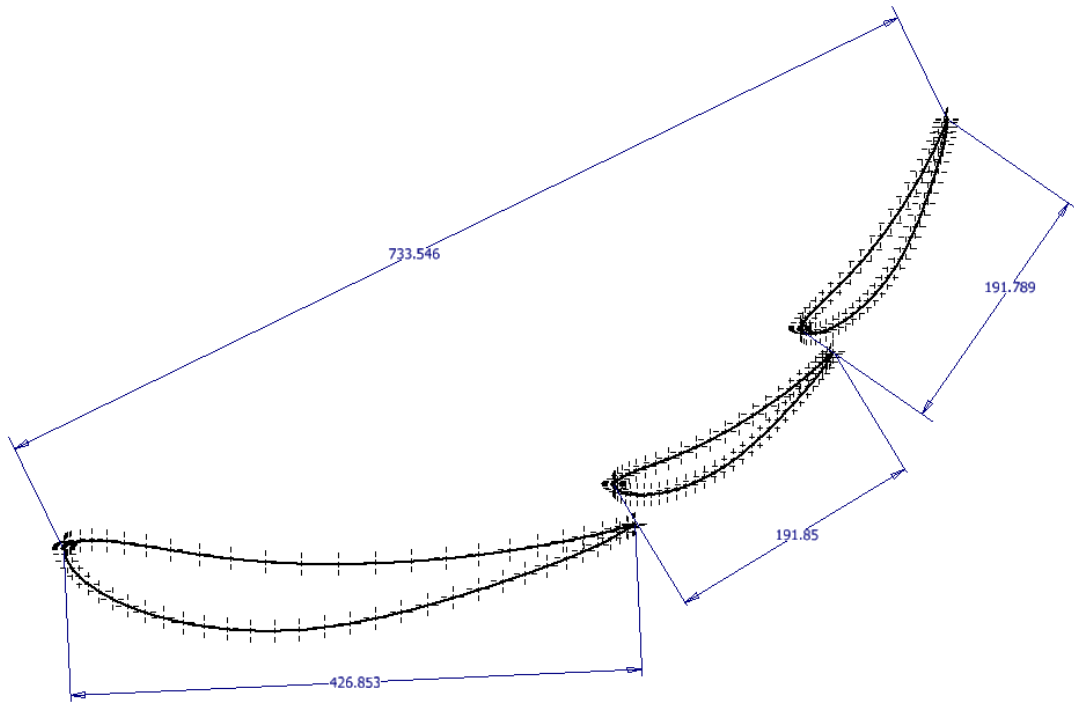


Figure 16: Aerofoil configuration from DoE optimisation

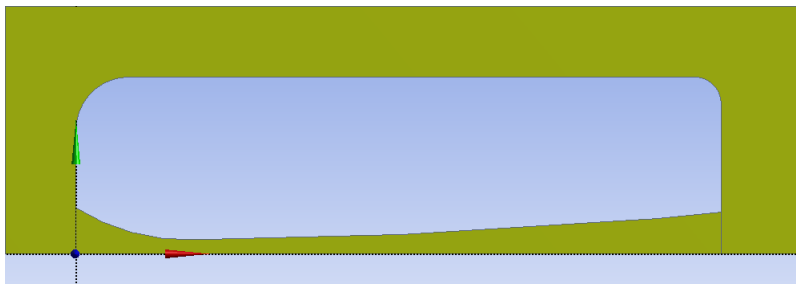


Figure 17: Undertray tunnel geometry with blunt body



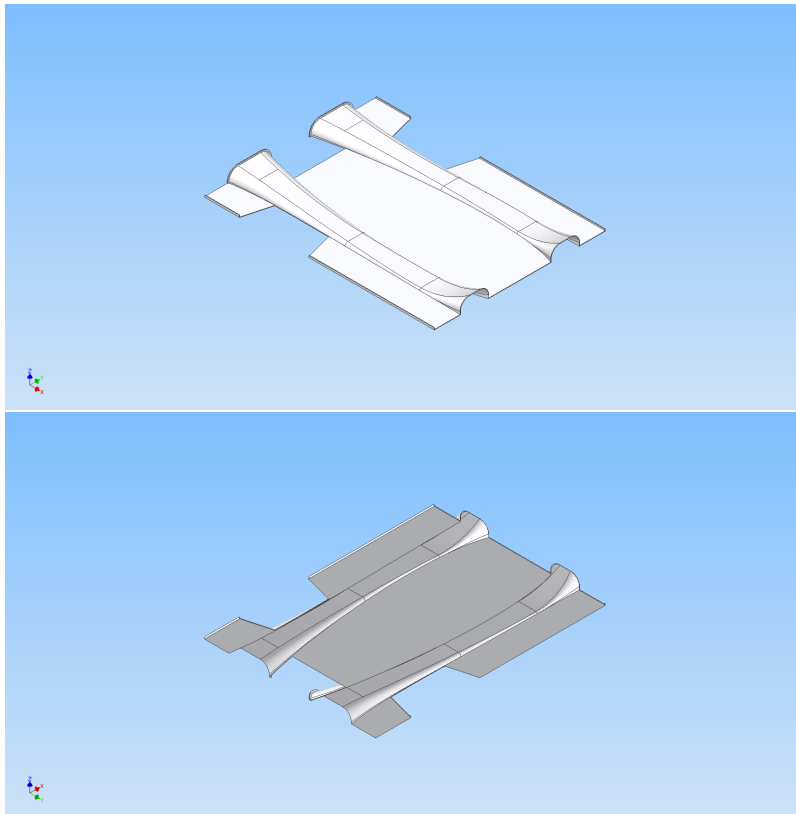


Figure 18: First revision of the undertray

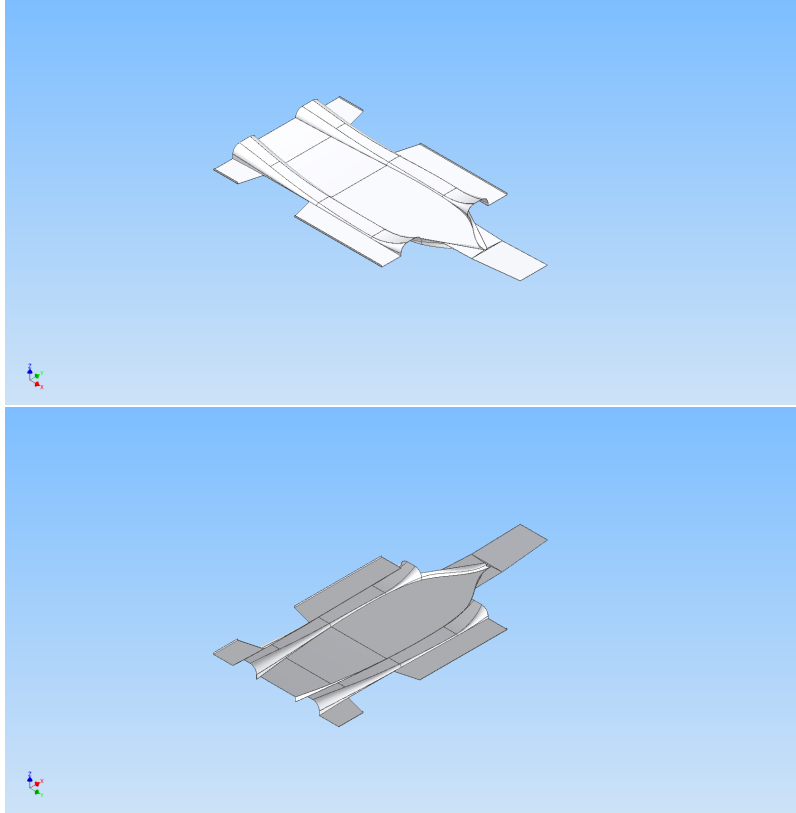


Figure 19: Second revision. Narrower diffuser tunnels and the added splitter and mounting section

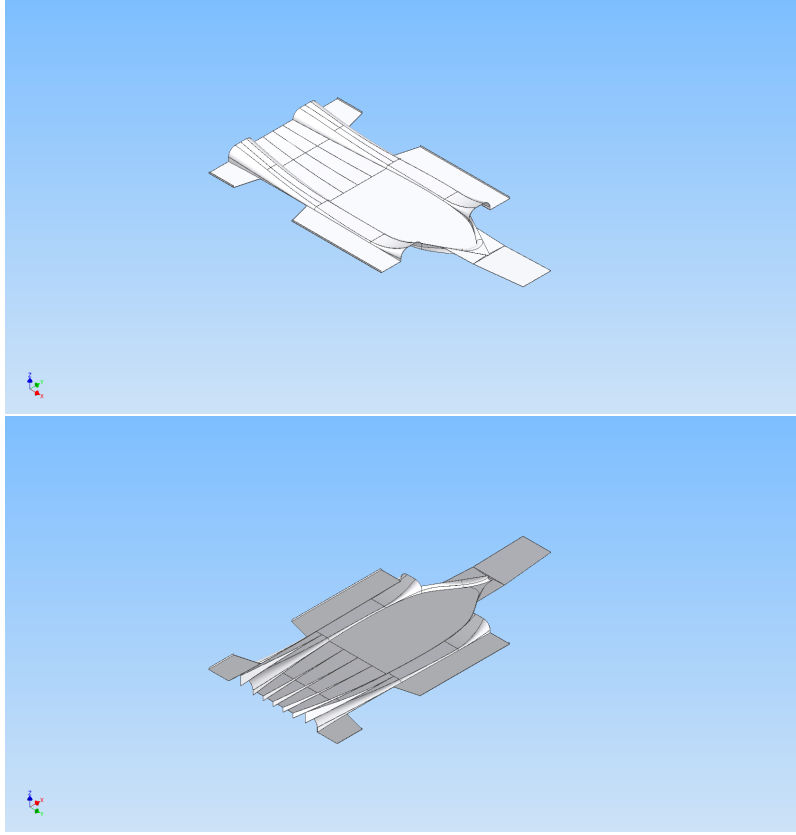


Figure 20: Final design with separation walls in the diffuser section

excluded from this project.

### 5.3 Wing simulation

To design the front wing for maximum downforce, the desire was to make it as large as the rules would allow while investigating the angle of attack and the clearance to the ground. The CFD simulations of the entire vehicle are very time-consuming however, and in order to save some time it was decided that the ground clearance should be set at 10% of the total coord as suggested in [4], while investigating the angle of attack. Three angles around the maximum for the 2D lift curve were chosen and simulated separately. The end plates at the tips of the wing were designed without any underlying analysis, solely based on inspiration from the many Australian Formula Student teams. The results from the simulations give limited insight into

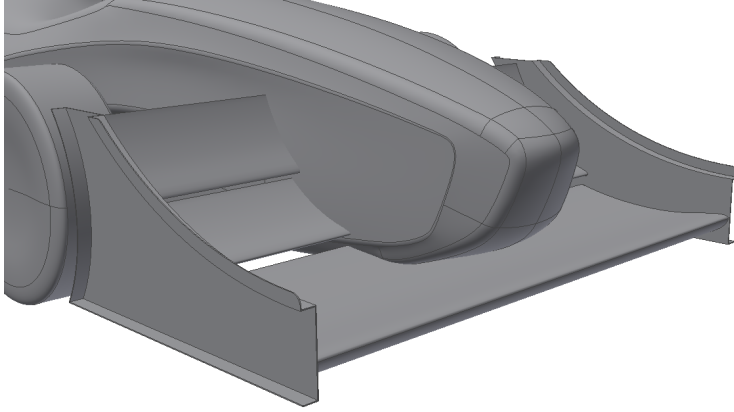


Figure 21: Front wing CFD model

$\alpha$	$C_L$
22	0.7345
24	0.7742
26	0.7811

Table 2:  $C_L$  for different angles of the front wing

the full behaviour of the front wing, but at the very least it indicates that there is a small range of angles where it can operate properly, and it shows that the performance is increasing up until at least an angle of  $26^\circ$ , as with the aerofoil in the 2D case. For the remainder of the simulations with the addition of the rear wing, the front wing was held at an angle of attack of  $26^\circ$ .

When the front wing simulations were completed it was time to put the rear wing in place. The process was tainted by mesh generation difficulties and time constraints, so the amount of simulations that could be run was limited. The wing was designed to be as large as possible, positioned over the rear wheels, and the simulations would then tell if the set-up needed to be adjusted to achieve the desired load distribution. Two simulations were run, one with an inlet air velocity at 17 m/s and another at 34 m/s to see how the load distribution changes at different velocities around the track. The center of pressure from all the aerodynamic forces acting on the vehicle was extracted from FLUENT and the load distribution derived from it in both cases.

While only slightly, it can be seen that the load is transferred forward at higher velocities, which indicates that the front wing works better than the rear wing, and seems to operate well in ground proximity. The desire was to have an even

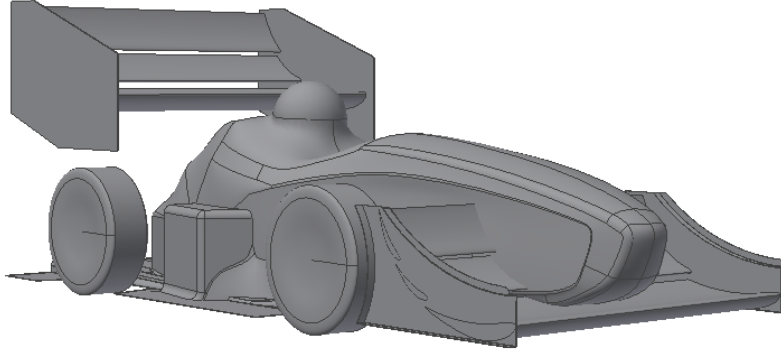
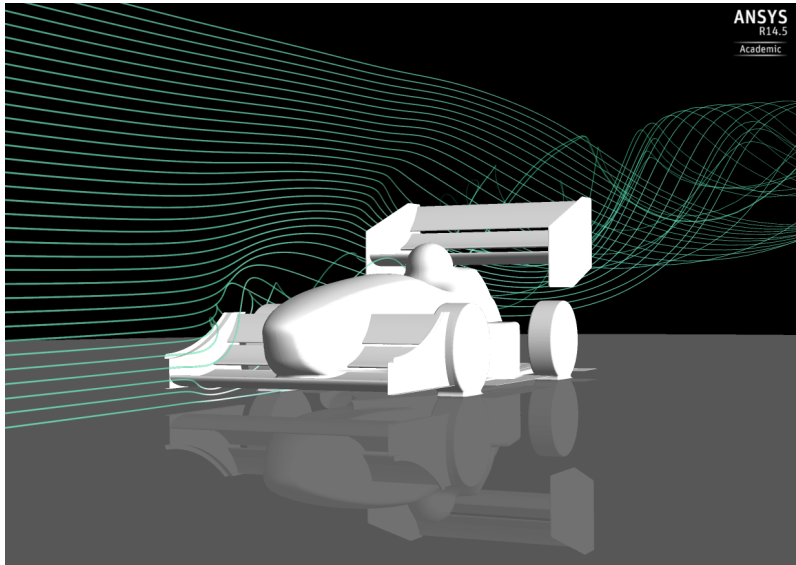


Figure 22: Complete CFD model with rear wing

Velocity [m/s]	Load distribution, Front - Rear
17	58.1% - 41.9%
34	59.6% - 40.4%

Table 3: Load distribution on tyres at different velocities

distribution between the front and rear tyres. It may be possible to modify the rear wing to produce more downforce to even out the balance, but as it was designed to be practically as big as possible, one may find better solutions by looking at adjusting the front wing. In these simulations, the front wing angle of attack was set to its expected maximum of  $26^\circ$ , as mentioned. This may not be desirable as the angle might increase momentarily during heavy braking before corners. If the angle of attack increases too much, leading to a separation, all downforce in the front will be lost, and the grip in the front tyres would be very poor when heading into the corner. This would obviously be bad for the performance of the vehicle in terms of getting around the track as quickly as possible, and it may be dangerous for the driver. For these reasons it should be better to reduce the angle of attack of the front wing, even though it will produce less downforce in total, to achieve the load distribution that is sought after. Another benefit to this approach is that the blockage from the front wing of the cooling system at the sides of the driver will be less severe. Ultimately, final tuning of the vehicle's balance is best done during the testing stages where one can use an experienced driver as a sensor to receive feedback on what changes and fine-tuning needs to be made.



## 6 Acknowledgements

I would like to thank my supervisor Stefan Wallin for sharing his invaluable experience and guidance through the course of this project. I would also like to thank Jonathan Zerihan, Maximillian Tomac, and Scott Wordley for their information about their previous projects in the field. Lastly, thanks to Gustav Amberg for letting me choose this subject for my thesis.

## References

- [1] S. S. Pakkam, *High Downforce Aerodynamics for Motorsports*. Raleigh, North Carolina, 2011.
- [2] S. McBeath, *Competition Car Downforce*, Haynes Publishers, 1998.
- [3] R. H. Bernard, *Road Vehicle Aerodynamic Design*, MechAero Publishing, 2nd edition, 2001.
- [4] J. Katz, *Race Car Aerodynamics*, Bentley Publishers, 1995.
- [5] S. Wordley, J. Saunders, *Aerodynamics for Formula SAE: Initial Design and Performance Prediction*, SAE Paper 2006-01-0806, 2006.
- [6] S. Wordley, J. Saunders, *Aerodynamics for Formula SAE: A Numerical, Wind Tunnel and On-Track Study*, SAE Paper 2006-01-0808, 2006.
- [7] SAE, *2014 Formula SAE Rules*, Society of Automotive Engineers, 2005.  
<http://students.sae.org/cds/formulaseries/rules/>
- [8] X. Zhang, J. Zerihan, *Aerodynamics of a Double Element Wing in Ground Effect*, AIAA Journal, Vol. 41, No. 6, pp 1007-1016, 2003.
- [9] D. Case, *Formula SAE: Competition History 1981-2004*, Society of Automotive Engineers, 2005.
- [10] UIUC Airfoil Coordinates Database,  
[http://aerospace.illinois.edu/m-selig/ads/coord\\_database.html](http://aerospace.illinois.edu/m-selig/ads/coord_database.html)
- [11] M. Lanfrit, *Best practice guidelines for handling Automotive External Aerodynamics with FLUENT*, Fluent Deutschland GmbH, 2005.